

Bio-inspired motifs via tandem assembly of polypeptides for mineralization of stable CaCO₃ structures

Gousia Begum *and* Rohit Kumar Rana*

Nanomaterials Laboratory, Inorganic and Physical Chemistry Division, Indian Institute of Chemical Technology, Hyderabad-500 607, India. E-mail: rkrana@iict.res.in

Supporting Information

Experimental:

Materials:

Penta(L-lysine hydrobromide) (penta(L-lys), 1-5 kDa), Poly(L-aspartic acid sodium salt) (poly(L-asp), 15-50 kDa and 5-15 kDa) and Fluorescein isothiocyanate (FITC) were procured from Sigma-Aldrich and were used as received. Calcium chloride (CaCl₂) and ammonium carbonate (NH₄)₂CO₃ were obtained from Qualigen Fine Chemicals, India. All the solutions were prepared using de-ionized water (18.2 MΩ, Millipore water purification system).

Methods:

Dye conjugation of poly(L-asp) with FITC: Typically 10 mg of poly(L-asp) was dissolved in 1 mL of 0.1M Na₂CO₃ buffer. To this 0.1 mL of FITC (5 mg of FITC dissolved in 0.5 mL of dimethylsulphoxide (DMSO)) was added. The mixture was kept at 4 °C for 24 h in the dark. The resulting solution was centrifuged using an Amicon centrifuge tube with 3 kDa molecular weight cut off to collect the FITC-tagged poly(L-asp) sample.

Dye conjugation of penta(L-lys) with FITC: Typically 0.4 mg of FITC was dissolved in 0.1 mL of dimethylsulphoxide (DMSO). In a separate container 50 mg of penta(L-lys) was dissolved in 1 mL of de-ionized water and the solution pH was adjusted to 8.4 using NaOH. The two solutions were combined and stirred for two days at room temperature in the dark. The FITC-tagged penta(L-lys) was then obtained by centrifuging the resulting solution using Amicon centrifuge tube with 3 kDa molecular weight cut off.

Synthesis of CaCO₃ microstructures: Calcium carbonate microstructures were prepared using poly(L-asp) (5-50 kDa) and penta(L-lys) (1-5 kDa) as both structure directing and mineralizing agents in liquid phase (Table 1). In a typical synthesis, to 200 μL poly(L-asp)(2-10 mg/mL), 200 μL of penta(L-lys) (2 mg/mL) was added which resulted in a turbid solution. This mixture was then aged for 30 min. To this salt polymer aggregate 200 μL of CaCl₂ (0.05-1M) was added

followed by addition of 200 μL of $(\text{NH}_4)_2\text{CO}_3$ (0.05-1M). This mixture was then aged for different time intervals of 30 min to 15 h at room temperature. The calcium carbonate precipitates then obtained were centrifuged at 9000 rpm and washed 5 – 6 times with de-ionized water and dried at room temperature. The charge ratio R (the ratio of number of positive charges on penta(L-lys) to the number of negative charges on poly(L-asp)) was ~ 0.7 (sample 1). A blank reaction was also carried out in absence of poly(L-asp) and penta(L-lys) keeping all other parameters same. Similarly, to study the effect of individual components, the reactions were carried out using either of the above mineralizing agents (Table S2).

Characterizations: Powder X-ray diffraction (XRD) pattern were recorded on a SIEMENS (Cheshire, UK) D5000 X-ray Diffractometer over a 2θ range of 2° to 60° using $\text{CuK}\alpha$ ($\lambda=1.5406\text{\AA}$) radiation at 40 kV and 30 mA with a standard monochromator using a Ni filter. High Resolution Transmission electron microscope (HRTEM) (JEOL TEM 2010 microscope operating at 200 kV) was used to investigate morphology and size of the particles. The samples for TEM were prepared by dispersing the material in ethanol by ultrasonication and drop drying onto a formvar coated copper grid. Scanning Electron Microscopic (SEM) analyses of the prepared materials were performed by using Hitachi S-3000N Scanning Electron Microscope. The confocal imaging was carried out under Leica Confocal System TCS SP5 with 63 X 1.4 NA objective and with a gain value of 850-950 V. Optical sectioning was done at 0.5 mm intervals with 1 AU pinhole and three of the central sections were projected using the LAS AF software. For FITC tagged samples, 488 nm laser line was used for excitation and the emissions were collected using 500-550 BP. FT-IR spectra of the solid samples were recorded on a Nicolet Nexus 670 spectrometer equipped with a DTGS KBr detector over range of 4000 cm^{-1} - 400 cm^{-1} . Confocal Micro Raman spectra were recorded using a Horiba Jobin-Yvon LabRam HR spectrometer with a 17 mW internal He Ne (Helium-Neon) laser source of excitation wavelength 632.8 nm. Dynamic Light Scattering (DLS) measurements were done with a Zetasizer 3000HSA (Malvern instruments, UK) using a 90° scattering angle and a laser light of wavelength 633 nm. The hydrodynamic diameters of particles were calculated by using the automated mode. The system was calibrated by using the $199 \pm 6\text{ nm}$ NanospheresTM Size Standard (Duke Scientific Corp., Palo Alto, CA, USA) and DTS 0050 standard from Malvern. Thermogravimetric analysis was done with Mettler Toledo star^c TG analyzer in N_2 atmosphere, with a heating rate of $10\text{ }^\circ\text{C}/\text{min}$ from $25\text{ }^\circ\text{C}$ to $1000\text{ }^\circ\text{C}$.

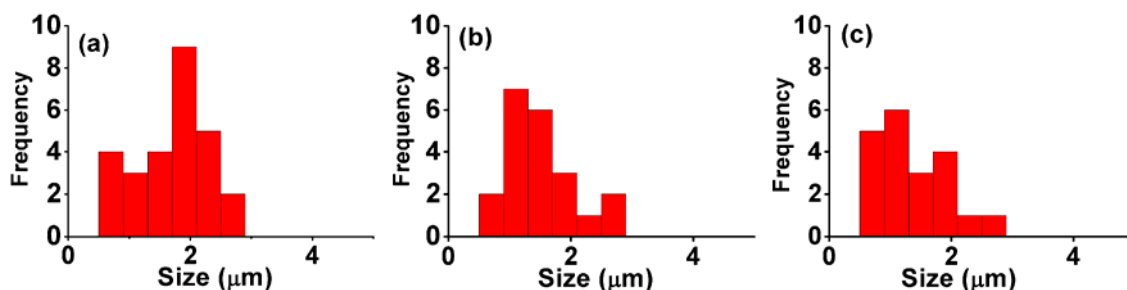


Fig. S1 DLS measurements to obtain size distribution of the particles in a colloidal form; Size distribution plots of the (a) aggregates formed after the addition of poly(L-asp) to penta(L-lys) aged for 30 min; (b) after addition of CaCl₂ to these aggregates; (c) after addition of (NH₄)₂CO₃ to these aggregates containing CaCl₂.

Table S1. Structural parameters of the CaCO₃ samples prepared using 0.5 mg/mL of each poly(L-asp) and penta(L-lys) for a reaction duration of 15 h.

Sample #	Shape ^a	Crystallite size, [nm] ^b
1.	Spherical	14.36
2.	Spherical	17.94
3.	Spherical	17.36
4.	Spherical	36.10
5.	Rhombohedra	36.09

^[a] Shape of the particles was determined by SEM and TEM.

^[b] Crystallite size were calculated from XRD using Debye–Scherrer formula, which is expressed as:

$$D = \frac{k\lambda}{\beta_{hkl} \cos \theta}$$

where ‘k’ is the shape factor constant that varies from 0.98 to 1.39, λ is the wavelength of X-rays, β_{hkl} is the full width at half maximum for a particular (hkl) value.

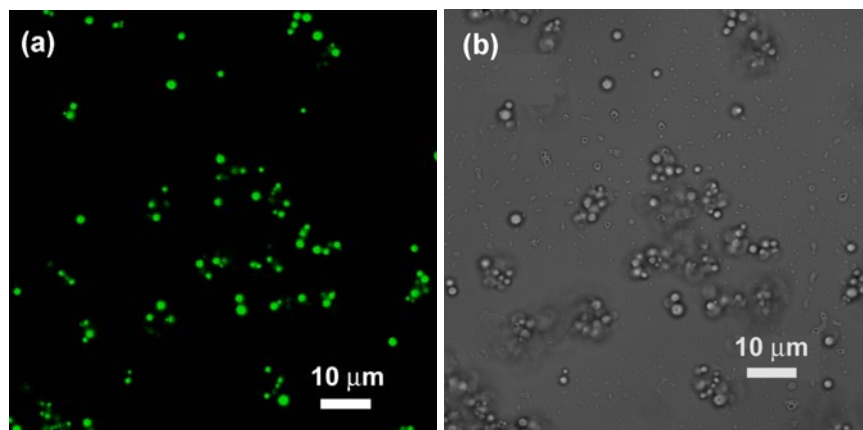


Fig. S2 (a) Confocal and (b) bright field images of CaCO₃ microspheres prepared in the presence of poly(L-asp) and penta(L-lys) (Sample 1).

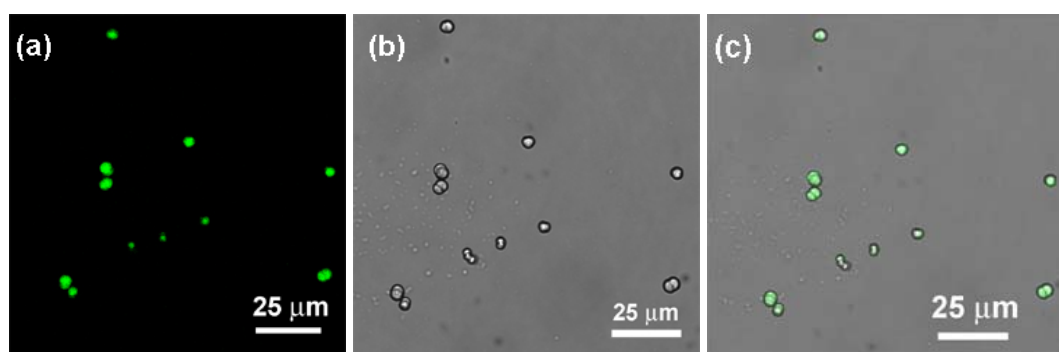


Fig. S3 Confocal microscopic analysis to illustrate the presence of penta(L-lys); The images correspond to (a) confocal fluorescent (b) bright-field and (c) overlay images of the Sample 1 prepared using FITC-tagged penta(L-lys).

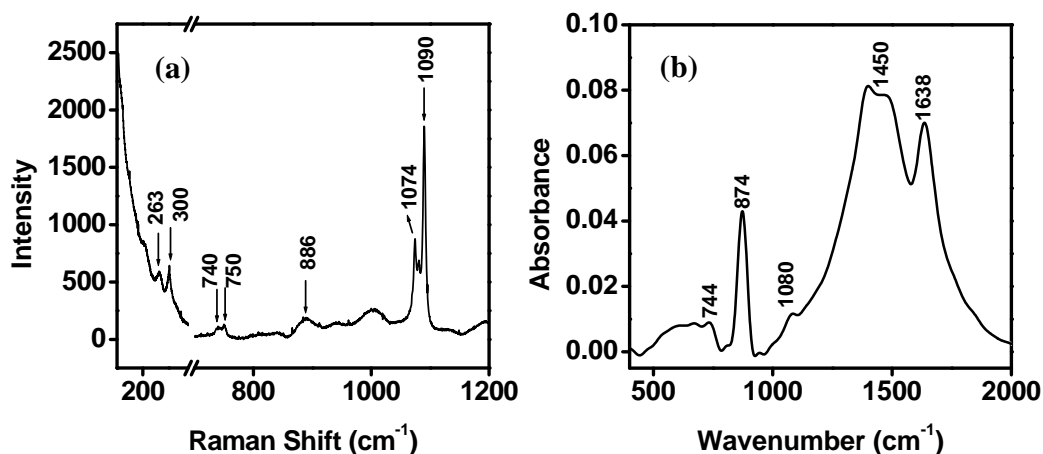


Fig. S4 (a) Micro-Raman and (b) FT-IR spectra of CaCO₃ microspheres prepared in the presence of poly(L-asp) and penta(L-lys) (Sample 1). The FT-IR spectrum shows the presence of polypeptides with an absorbance at 1638 cm⁻¹ due to the amide linkages (CONH).

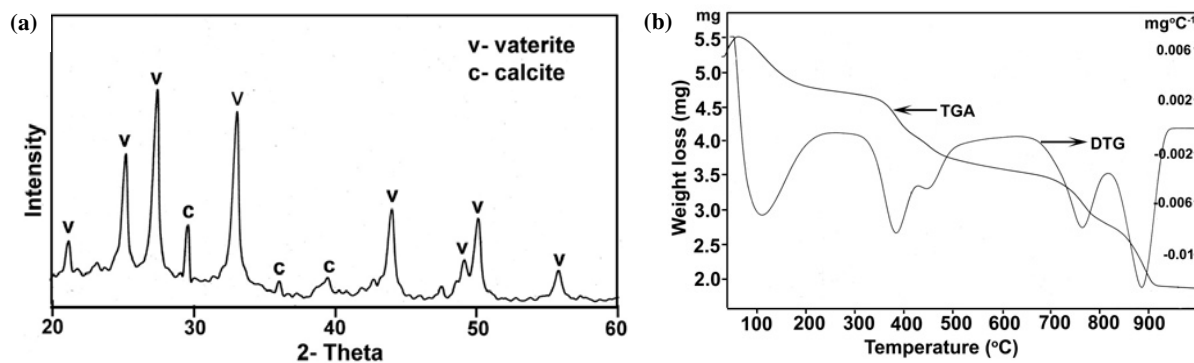


Fig. S5 (a) XRD pattern of CaCO_3 microspheres prepared in the presence of poly(L-asp) and penta(L-lys) and (b) TGA spectrum of the CaCO_3 microstructures prepared in the presence of poly(L-asp) and penta(L-lys) (Sample 1). The sample was aged for 15 h.

Thermo Gravimetric Analysis (TGA): For the Sample 1 the organic content in the CaCO_3 spheres is about 15.22 wt. % as estimated from TGA (Fig. S5(b)). The percentage of CaCO_3 present in the microspheres correspond to ~81 wt. % and rest 3.6 wt. % is water. Theoretically, CaCO_3 loses 44% of weight due to decomposition of CaCO_3 to CO_2 and CaO . The wt. % of poly(L-asp) and penta(L-lys) incorporated into the CaCO_3 microspheres was obtained by subtracting the weight lost by decomposition of CaCO_3 and water from the total weight lost at 900 °C. The yield of the sample aged for 30 minutes was found to be 30.14% as calculated by weight of CaO from TGA analysis compared to the theoretical weight and it increased to 43.21% for the same sample aged for 15 h (Fig. S5(b)).

Morphogenesis of the CaCO₃ structure with change in concentration of Ca²⁺ and CO₃²⁻ ions: The increase in the precursor concentration also resulted in increase in the calcite phase while the percentage of vaterite decreased from 83.4% to 21.7%. The gradual increase in calcite percentage suggests that the excess of Ca²⁺ ions which doesn't interact with the polypeptides lead to formation of such phases. Formation of the rhombohedral shapes which nearly resembles the shapes of calcite formed without any additives (Fig. 4a, Sample 8), further supports the above fact and the excess Ca²⁺ ions are deposited on the surface of the initially formed spherical particles as calcite phase.

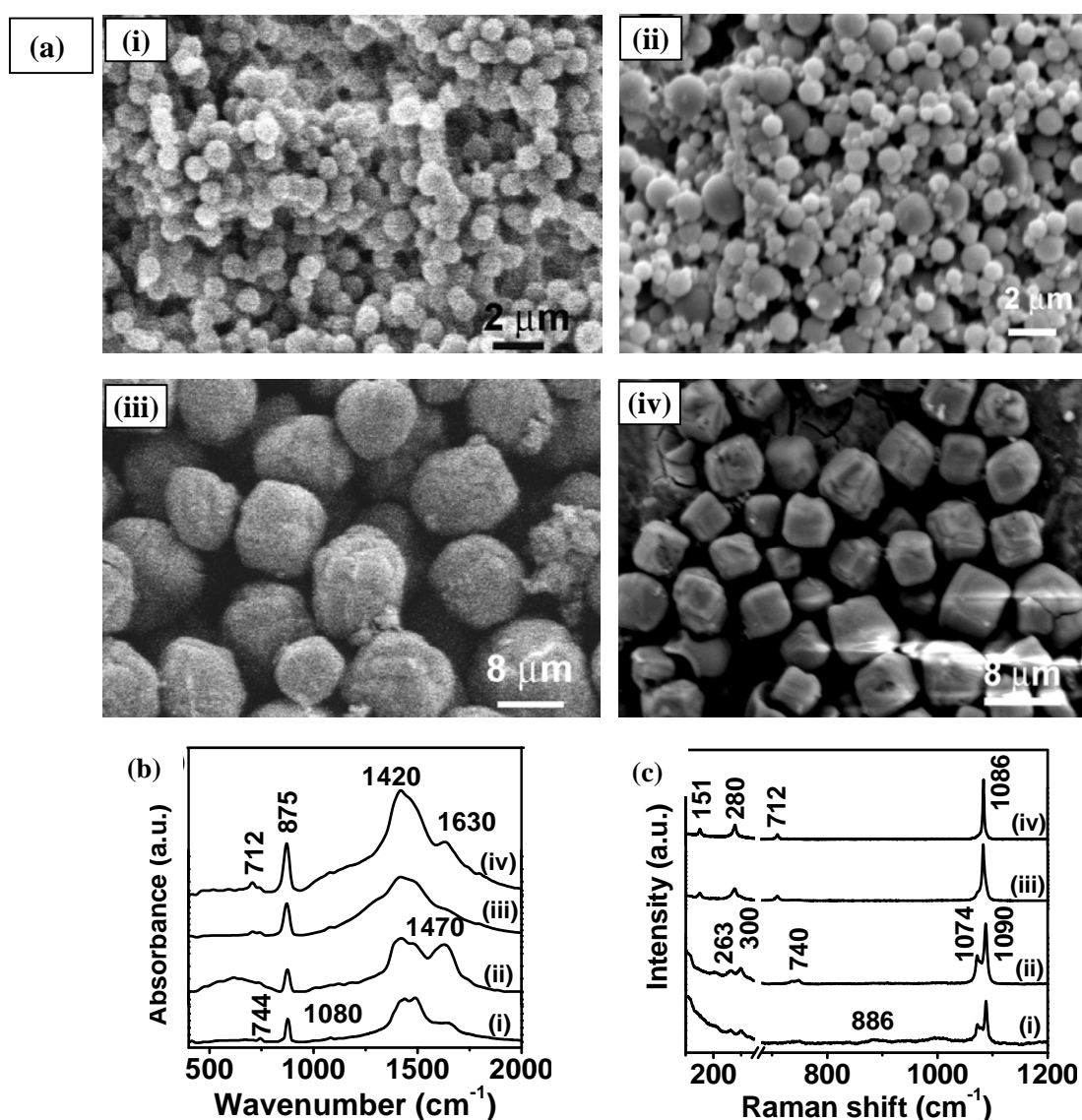


Fig. S6 (a) SEM images (b) FT-IR and (c) Micro-Raman spectra of CaCO₃ microstructures prepared in the presence of poly(L-asp) and penta(L-lys); (i) Sample 2; (ii) Sample 3; (iii) Sample 4 and (iv) Sample 5.

Control Experiments:

Table S2. Structural parameters of the samples obtained in various control experiments using $[\text{Ca}^{2+}] = [\text{CO}_3^{2-}] = 0.0125 \text{ M}$ for a reaction duration of 15 hr.

Sample #	Mineralizing agent	Polymorphism and (Vaterite fraction) ^[a]	Shape ^[b]	Crystallite size ^[c] , [nm]
6.	Penta(L-lys)	Calcite	distorted rhombohedral	37.86
7.	Poly(asp)	Vaterite(0.6273)*+ Calcite	spherical+ irregular	19.92
8.	-	Calcite	rhombohedral	47.33

^[a]Fraction of vaterite was estimated from XRD peak intensity using the Rao's equation: $f_v = [I_{110(v)} + I_{112(v)} + I_{114(v)}] / [I_{110(v)} + I_{112(v)} + I_{114(v)} + I_{104(c)}]$, where f_v indicates fraction of vaterite in the sample. ^[b] Shape of the particles was determined by SEM and TEM. “*” Indicates the polymorph which is in excess if more than one form exists. ^[c] Crystallite size were calculated from XRD using Debye–Scherrer formula.

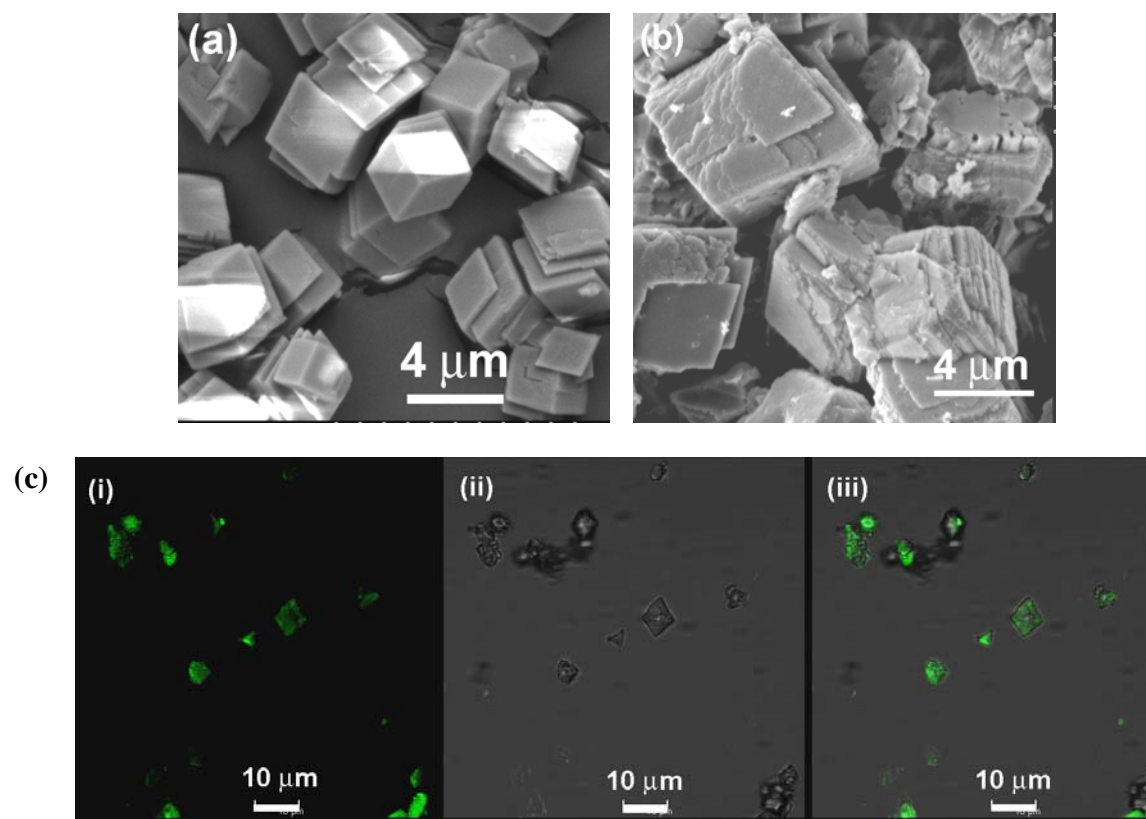


Fig. S7 (a) & (c) SEM confocal images of calcite rhombohedra with truncated edges prepared in the presence of penta(L-lys); (b) SEM image of calcite prepared without using any mineralizer.

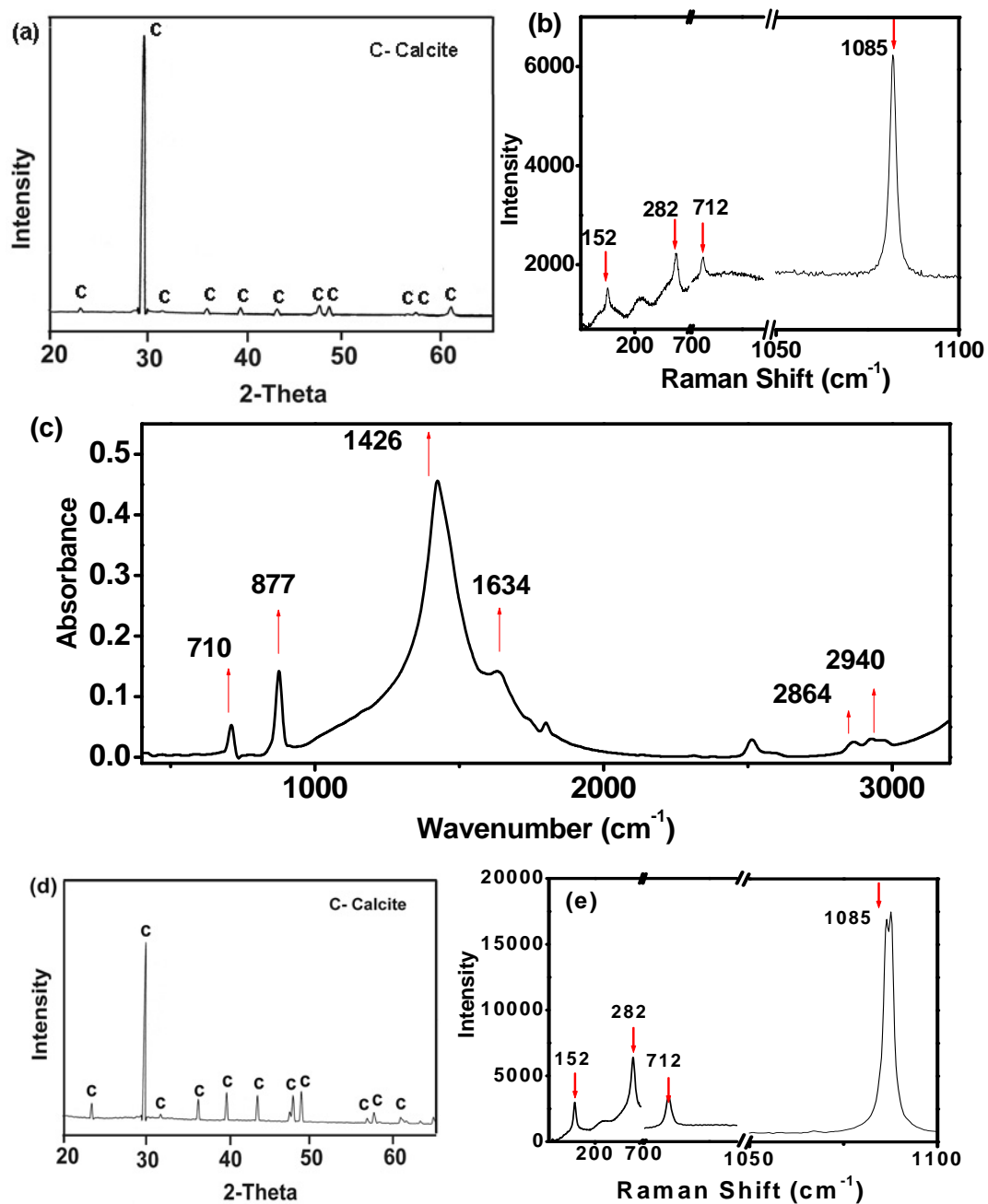


Fig. S8 (a) XRD pattern, (b) Raman spectra, (c) FT-IR spectrum of calcite rhombohedra with truncated edges (Sample 6) prepared in presence of only penta(L-lys), (d) XRD pattern and (e) Raman spectra of calcite rhombohedra prepared in the absence of any of the additives (Sample 8). All the samples were aged for 15 h.

The XRD patterns of Sample 6 (Fig. S8(a)) prepared in the presence of only penta(L-lys)) and Sample 8 (Fig. S8(d)) prepared in the absence of any additives displayed characteristic reflections for calcite phase (JCPDS Card No. 05-0586). The Raman spectra of Sample 6 and

Sample 8 displayed bands at 152, 282 and 712 cm^{-1} in addition to a sharp band at 1085 cm^{-1} which are characteristics for the calcite phase (Fig. S8(b) & (e)).^{1,2} The bands at 152 and 282 cm^{-1} are due to lattice modes and a band at 712 cm^{-1} is attributed to ν_4 in-plane bending mode of carbonate internal vibrations. Also a band at 1085 cm^{-1} is assigned to ν_1 symmetric stretching vibration of carbonate group. In addition to bands at 1426 and 877 the FT-IR spectra of sample 6 exhibited peak at 710 cm^{-1} indicating the calcite polymorph. Also the presence of peaks at 2940 and 2864 cm^{-1} due to asymmetric and symmetric vibrations of methylene groups respectively indicates the presence of penta(L-lys) chains in the CaCO_3 matrix (Fig. S8(c)).

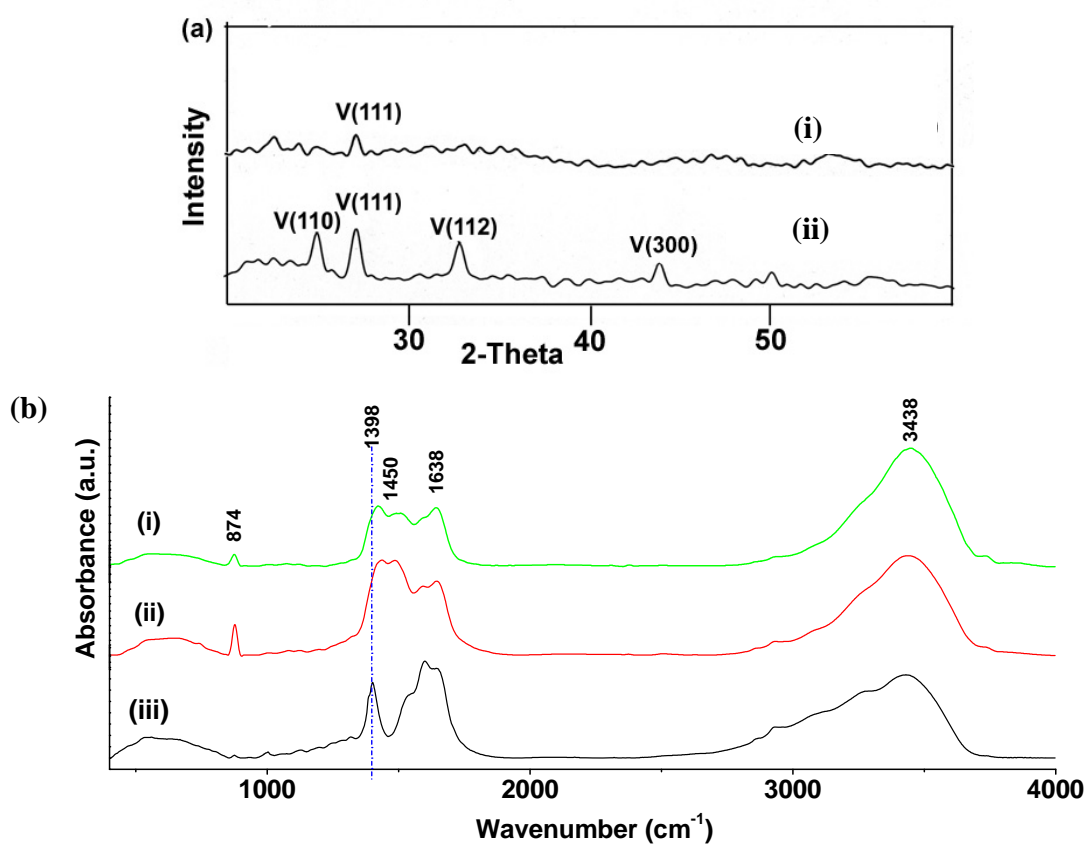


Fig. S9 (a) XRD patterns and (b) FT-IR spectra of the samples prepared by increasing the concentration of poly(L-asp) to (i) ten and (ii) four times the value in Sample 1. The samples were aged for 15 h. FT-IR spectrum of (iii) a mixture of poly(L-asp) and penta (L-lys) is also given in (b) for comparison. The FT-IR spectrum of a physical mixture of poly(L-asp) and penta (L-lys) exhibited an absorbance at 1398 cm^{-1} attributed to the symmetric stretching of carboxylate groups. There is also the signature of amide linkage (CONH) present in both poly(L-asp) and penta(L-lys) which has an absorbance at 1638 cm^{-1} .

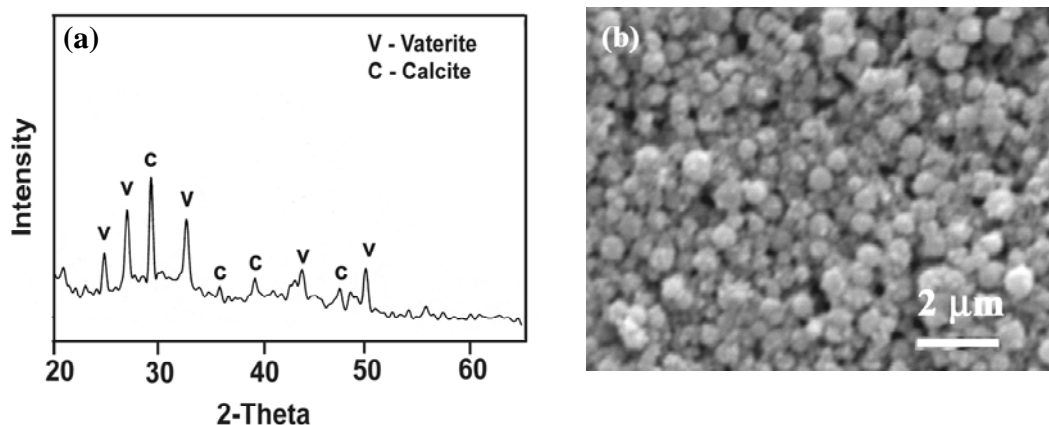


Fig. S10 (a) XRD pattern and (b) SEM image of Sample 7 (prepared in presence of only poly(L-asp)) with an ageing time of 15 h.

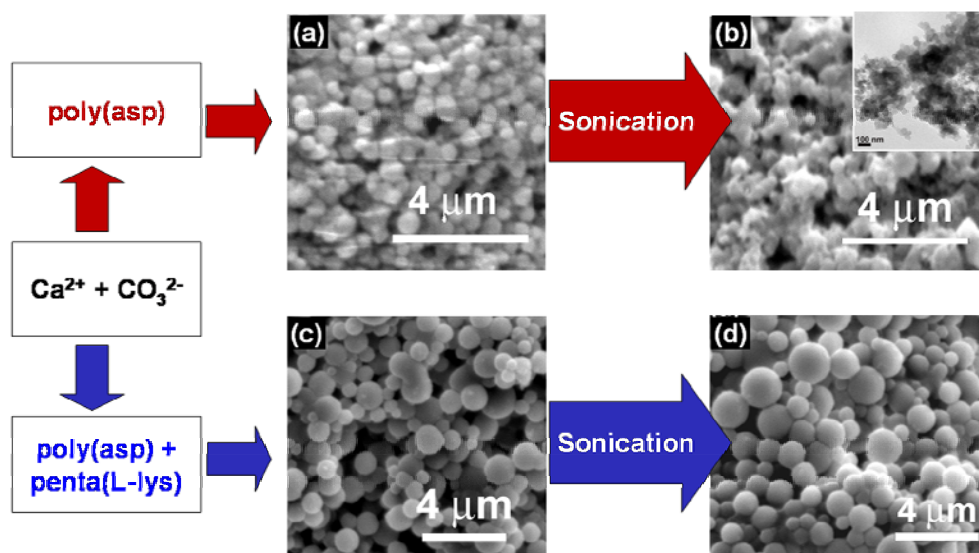


Fig. S11 Schematic illustration of the stability of the CaCO₃ microspheres. SEM images of the samples prepared using poly(L-asp) as the mineralizer in (a) absence (Sample 7) and (c) presence (Sample 1) of penta(L-lys), which under sonication transform to materials as shown in the SEM images (b) Sample 7 (inset TEM image) and (d) Sample 1 respectively.

References:

1. S. P. S. Porto, J. A. Giordmaine and T. C. Damen, *Phys. Rev.* 1966, **147**, 608.
2. C. Gabrielli, R. Jaouhari, S. Joiret, G. Maurin, *J. Raman Spectrosc.* 2000, **31**, 497.